Sub-THz Electromagnetic Wave Interactions with Ferroelectric Polarization Vortex Lattices

M. Degen[1], V. Jandieri[1], R. Khomeriki[2], and D. Erni[1]

[1] *General and Theoretical Electrical Engineering (ATE), University of Duisburg-Essen (UDE), and Center for Nanointegration Duisburg-Essen (CENIDE), D-47048 Duisburg, Germany,* {*marvin.degen, vakhtang.jandieri, daniel.erni*}*@uni-due.de*
[2] *Physics Department, Tbilisi State University, 3 Chavchavadze, 0128 Tbilisi, Georgia, ramaz.khomeriki@tsu.ge*

Ferroelectric materials are a subset of pyroelectric materials that both exhibit spontaneous polarization. In contrast to pyroelectric materials, the spontaneous polarization in bulk ferroelectric materials depends on the history of the external applied electric field, similar how the magnetization in ferromagnetic materials is influenced by external magnetic fields. Therefore, technical applications of ferroelectric materials can be found e.g. in non-volatile memory devices. Experimental observations [1] have shown that stacking alternating thin layers of ferroelectric and paraelectric materials leads to the evolution of meta-stable chiral polarization vortex lattices within the ferroelectric layers as schematically shown in Figure 1 for lead-titanate $PbTiO_3$ (PTO) as ferroelectric and strontium-titanate $SrTiO_3$ (STO) as paraelectric material. Under illumination of an external electric field, a frequency response of these material systems in the sub-THz regime has been observed [2].

Phenomenologically, this behavior can be analyzed by phase-field models minimizing the free energy of the system governed by a second-order time-dependent Landau-Ginzburg-Devonshire

This work was supported by the Deutsche Forschungsgemeinschaft (DFG) through CRC/TRR 196 MARIE (287022738) under project M03.

(TD-LGD) equation coupled to the electrostatic equilibrium equation [3, 4]

$$\mu\ddot{P}_i + \gamma\dot{P}_i = -\frac{\delta F}{\delta P_i}, \tag{1a}$$

$$\varepsilon_0\varepsilon_\mathrm{r}\Delta\varphi = \nabla\cdot\boldsymbol{P}, \tag{1b}$$

where P_i is the i-th component of the polarization vector $\boldsymbol{P}$, μ is the effective polarization mass density, γ is a damping coefficient, φ is the electric potential, ε_0 and ε_r are the vacuum and relative permittivity, respectively, and F is the free energy functional of the system. Taking into account Landau, gradient, and electrostatic energy contributions, and implying Einstein summation convention, the free energy functional is written as

$$F = \int_V \Big[\alpha_{ij}P_iP_j + \alpha_{ijk\ell}P_jP_jP_kP_\ell + \alpha_{ijk\ell mn}P_iP_jP_kP_\ell P_mP_n + \frac{1}{2}g_{ijk\ell}\frac{\partial P_i}{\partial x_j}\frac{\partial P_k}{\partial x_\ell} - \frac{1}{2}\varepsilon_0\varepsilon_\mathrm{r}E_iE_i - E_iP_i\Big]\,\mathrm{d}V, \tag{2}$$

where $\alpha_{\ldots}$ and $g_{ijk\ell}$ are the Landau and gradient energy coefficients, respectively, and E_i is the i-th component of the electric field vector $\boldsymbol{E} = -\nabla\varphi$. It is important to note that the mechanical displacement $\boldsymbol{u}$ can be included in the model by adding the corresponding energy contributions to the free energy functional and solving the mechanical equilibrium equation, which is coupled to the TD-LGD through electro-mechanical coupling terms typically caused by the electrostrictive effect. This also allows for taking into account lattice mismatch between the ferroelectric and paraelectric layers, which influences the structure of the vortex patterns [2]. Additionally, Maxwell's equations can be used requiring the electric and magnetic field $\boldsymbol{E}$ and $\boldsymbol{H}$ as dependent variables replacing the electric potential φ caused by the electrostatic equation [5].

However, here we will focus on the simplest case. To obtain a simple vortex pattern in the ferroelectric layers, accounting for Landau and gradient energy contributions is sufficient: in the paraelectric layers, all Landau coefficients are positive values, yielding a zero spontaneous polarization in the energy favorable

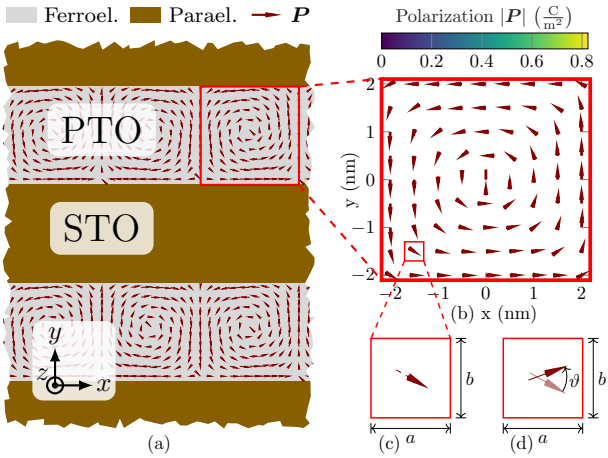

Figure 1: (a) Material system under investigation composed of alternating layers of ferroelectric PTO (gray) and paraelectric STO (brown), where polarization vortex patterns are formed in the ferroelectric material. (b) Magnification of a single vortex. The background color indicates the magnitude of the polarization vector field, while the arrows indicate its direction. (c) Schematic view of a single crystal unit-cell with dimensions a, b, and c (not shown) in x, y, and z-direction, respectively. The arrow indicates the corresponding dipole moment. (d) Dipole shown in the unit cell (c) deflected by an angle ϑ from its equilibrium position.

state in a bulk material. Contrary, in the ferroelectric layers, the first-order Landau coefficients are typically negative, while the higher-order coefficients are positive, yielding a non-zero spontaneous polarization as the energy favorable state. Therefore, at the interface between the ferroelectric and paraelectric layers, it is clear that the polarization vector field changes compared to its bulk behavior in order to mitigate large gradient energy contributions. Solving numerically the governing equations thus leads to the formation of the vortex pattern illustrated in Figure 1(a)

and (b).

Once the vortex pattern is formed, the coupling to an external electric field can be investigated by considering the electric field as a superposition of the external and internal field, i.e. $\boldsymbol{E} = \boldsymbol{E}_{\text{ext}} + \boldsymbol{E}_{\text{int}}$, and solving the governing equations. However, this is computationally expensive since the governing equation (1a) is non-linear requiring a solution in the time domain. Additionally, only limited physical insight is gained since the free energy functional (2) is a phenomenological expression and does not cover the actual physical processes in the material system. The former can be overcome by limiting the analysis to small perturbations around the equilibrium state subsequently allowing linearization, thus, leading to faster solutions in the frequency domain [6].

To gain physical insight into the underlying dynamics, we developed a torsional oscillator model [7] and extended it towards a torsional spring model [8]: in case of PTO as ferroelectric material, each dipole in the vortex is caused by a mechanical displacement of the lead cations with effective charge q_{eff} through a distance $\Delta\boldsymbol{r}$ as is shown in Fig. 2(a). The polarization vector $\boldsymbol{P}$ can thus be written as

$$\boldsymbol{P} = \frac{\boldsymbol{d}}{V} = \frac{q_{\text{eff}}\,\Delta\boldsymbol{r}}{V}, \tag{3}$$

where $\boldsymbol{d} = q_{\text{eff}}\,\Delta\boldsymbol{r}$ is the dipole moment and $V = a\,b\,c$ is the volume of a crystal unit cell with site-lengths a, b, and c. Assuming the dipole as a pendulum with its fixed point at the unit cell center (cf. Fig. 2(b)), its moment of inertia I_z can be written as

$$I_z = m_{\text{Pb}}|\Delta\boldsymbol{r}|^2 = \frac{m_{\text{Pb}}V^2}{q_{\text{eff}}}|\boldsymbol{P}|^2, \tag{4}$$

where the last expression is obtained by using (3). Based on (4), one can now write the equation of motion for the dipole coupled to an external electric field as detailed in [7]. The subsequently obtained permittivity matrix can then be used to analyze the scattering of electromagnetic waves by the vortex pattern using

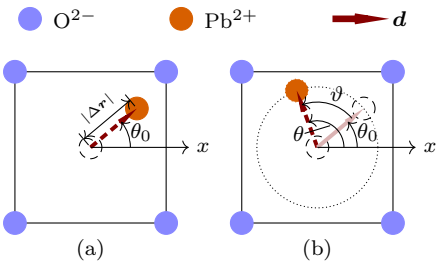

Figure 2: A single crystal unit cell with a dipole moment $\boldsymbol{d}$ caused by the displacement of the lead cation (orange) by $\boldsymbol{\Delta r}$. (a) shows the equilibrium state, where the angle between the dipole moment and the x-axis is θ_0. (b) depicts the deflected state, where the dipole moment is deflected by an angle ϑ from its equilibrium position.

e.g. the rigorous coupled wave method (approximating the vortex to be quadratic) or the T-matrix method combined with the Lattice-sums technique (approximating the vortex to be circular) [7].

The models described above neglect the systems endeavor to revert the equilibrium state yielding a restoring force acting on each deflected dipole. To account for the restoring force, a torsional spring can be assumed to be attached to each dipolar pendulum. Neglecting the mutual coupling between the dipoles, the principal of virtual work allows for estimating the restoring torque acting on each dipole when deflected by a small angle ϑ_i (cf. Fig. 2 (b)) as [8]

$$M_{\mathrm{res}}(\vartheta_i) \approx \frac{F_{\vartheta_i} - F_{\vartheta_{i-1}}}{\vartheta_i - \vartheta_{i-1}} \frac{V}{V_{\mathrm{C}}}, \tag{5}$$

where V and V_{C} are the volume of the crystal unit cell and its associated computational cell, respectively. Here, F_{ϑ_i} is the free energy of the system when the dipole under consideration is deflected by an angle ϑ_i while all other dipoles remain in their equilibrium state. The spring constant k can then be estimated

as

$$k \approx \frac{M_{\mathrm{res}}(\vartheta_i) - M_{\mathrm{res}}(\vartheta_{i-1})}{\vartheta_i - \vartheta_{i-1}}, \tag{6}$$

allowing for setting up a governing equation for the torsional spring model with the electric field causing the driving torque [8]. Although the model is simple, i.e. the coupling between the dipoles is neglected, the eigenfrequencies of all torsional-spring dipole models are found to be located between 0.16 THz and 0.50 THz which is in a good agreement with experimentally observed eigenfrequencies at 0.3 THz [2, 8]. Such surprisingly low frequencies open up completely new potential applications in the sub-THz regime such as the design of filter and metasurfaces which might be even electrically tunable by influencing the vortex structure through an external electric field. To obtain a more sophisticated model allowing even for modal analysis, the coupling between the dipoles caused by the gradient energy contribution needs to be taken into account through coupling springs between the torsional pendulums, which is currently under our consideration.

References

[1] A. K. Yadav *et al.*, "Observation of polar vortices in oxide superlattices," Nature, vol. 530, no. 7589, pp. 198–201, Feb. 2016.

[2] Q. Li *et al.*, "Subterahertz collective dynamics of polar vortices," *Nature*, vol. 592, no. 7854, pp. 376–380, Apr. 2021.

[3] T. Yang, B. Wang, J.-M. Hu, and L.-Q. Chen, "Domain Dynamics under Ultrafast Electric-Field Pulses," *Phys. Rev. Lett.*, vol. 124, no. 10, p. 107601, Mar. 2020.

[4] M. Degen, V. Jandieri, J. T. Svejda, and D. Erni, "Numerical Modeling of Polarization Vortex Evolution in Strained Ferroelectrics," in *Mikrosystemtechnik Kongress 2025*, Duisburg, Germany, Oct. 2025, pp. 130–131.

[5] M. Degen, R. Khomeriki, V. Jandieri, J. T. Svejda, P. L. Werner, D. H. Werner, J. Berakdar, and D. Erni, "Modeling Electromagnetic Wave Interactions with Ferroelectric Vortex Lattices in the Sub-THz Regime," in *15th International Conference on Metamaterials, Photonic Crystals and Plasmonics (META)*, Torremolinos, Spain, Jul. 2025, pp. 504-505.

[6] S. Zheng, J. Zhang, A. Li, and J. Wang, "Origin of Chiral Phase Transition of Polar Vortex in Ferroelectric/Dielectric Superlattices," *Nano Lett.*, vol. 25, no. 4, pp. 1397–1403, Jan. 2025.

[7] R. Khomeriki, V. Jandieri, K. Watanabe, D. Erni, D. H. Werner, M. Alexe, and J. Berakdar, "Photonic ferroelectric vortex lattice," *Phys. Rev. B*, vol. 109, no. 4, p. 045428, Jan. 2024.

[8] M. Degen, J. T., Svejda, V. Jandieri, R. Khomeriki, D. H. Werner, J. Berakdar, and D. Erni, "Exploring Dipole Dynamics in Ferroelectric Vortex Lattices: A Torsional Spring-Based Model," in *Int. Conf. Mobile and Miniaturized THz Systems (ICMMTS 2026)*, Jul. 2026, accepted.

Sub-THz Electromagnetic Wave Interactions with Ferroelectric Polarization Vortex Lattices

Marvin Degen, Vakhtang Jandieri, Ramaz Khomeriki, Daniel Erni

UNIVERSITÄT DUISBURG ESSEN
Offen im Denken

M. Degen | Bremen Workshop on Light Scattering 2026 | March, 17th 2026

UNIVERSITÄT DUISBURG ESSEN
Offen im Denken

Outline

- Ferroelectrics and ferroelectric vortex lattices
- Phase field model
- Torsional rotator model
- Square and circular vortex model
- Torsional spring model
- Perturbation analysis
- Conclusion and outlook

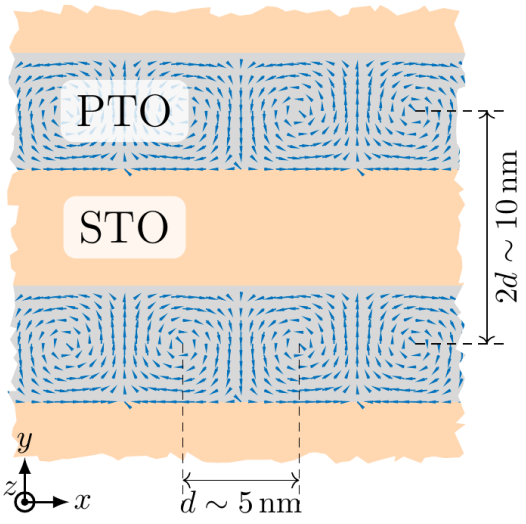

UNIVERSITÄT DUISBURG ESSEN

Offen im Denken

Ferroelectrics and Ferroelectric Vortex Lattices

- Pyroelectric: spontaneous polarization $\boldsymbol{P}_S \neq 0$
- Ferroelectric: hysteresis in *P-E* characteristic
  - Non-volatile memory
- Strong electrostrictive effect
  - Actuators

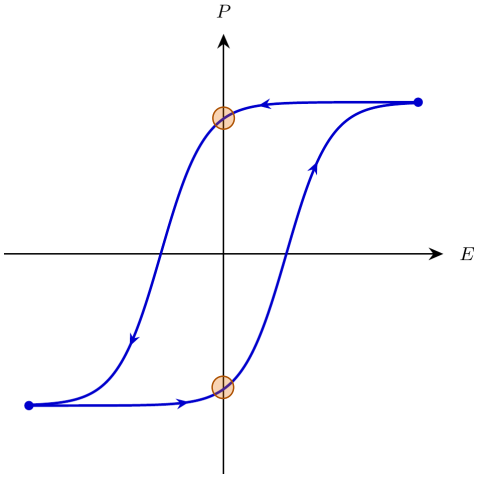

UNIVERSITÄT DUISBURG ESSEN

Offen im Denken

Ferroelectrics and Ferroelectric Vortex Lattices

- Pyroelectric: spontaneous polarization $\boldsymbol{P}_S \neq 0$
- Ferroelectric: hysteresis in *P-E* characteristic
  - Non-volatile memory
- Strong electrostrictive effect
  - Actuators
- **Topological structures in stacks of thin layers of ferroelectric and paraelectric material**

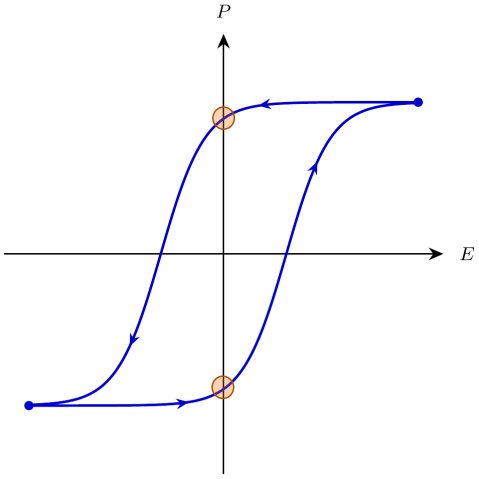

Ferroelectrics and Ferroelectric Vortex Lattices

- Strained alternating perovskite layers:
  - Lead titanate ($PbTiO_3$, PTO)
  - Strontium titanate ($SrTiO_3$, STO)
- Curie-temperature
  - $T_{C,STO} < T$ (paraelectric)
  - $T_{C,PTO} > T$ (ferroelectric)

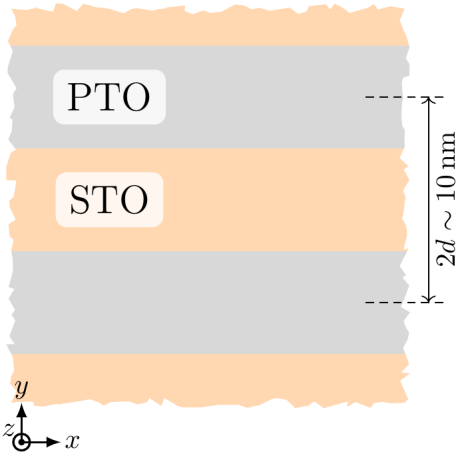

Ferroelectrics and Ferroelectric Vortex Lattices

- Strained alternating perovskite layers:
  - Lead titanate ($PbTiO_3$, PTO)
  - Strontium titanate ($SrTiO_3$, STO)
- Curie-temperature
  - $T_{C,STO} < T$ (paraelectric)
  - $T_{C,PTO} > T$ (ferroelectric)

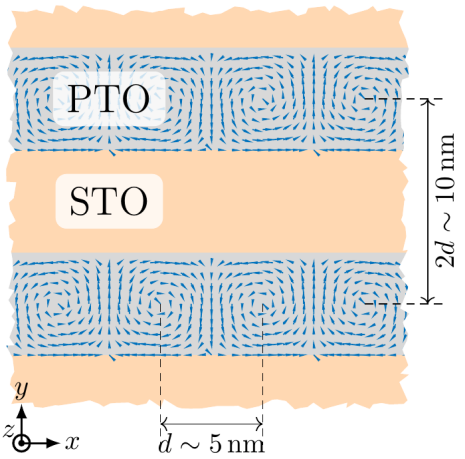

(Meta) stable state: local **energy minimum**

Ferroelectrics and Ferroelectric Vortex Lattices

- TEM microscopy: monitoring cation displacement → $\boldsymbol{P}$

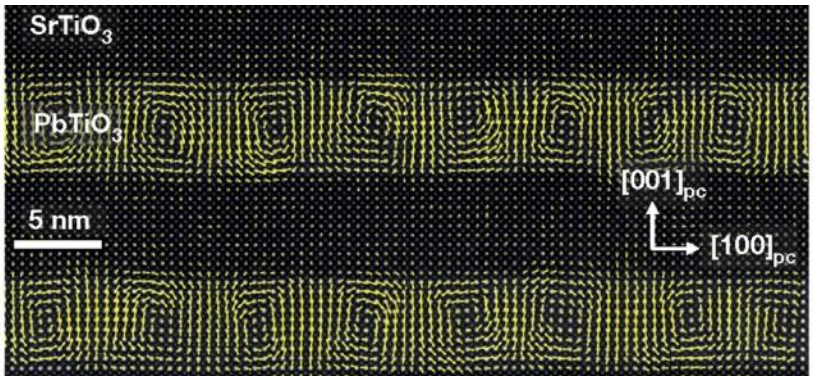

[1] A. K. Yadav *et al.*, *Nature*, vol. 530, no. 7589, 2016.

Phase Field Model

- Governing equations [1, 2]:

$\mu\ddot{P}_i + \gamma\dot{P}_i = -\frac{\delta F}{\delta P_i}$ (2nd-order TD-LGD equation)

$\rho\ddot{u}_i + \beta\rho\dot{u}_i = \nabla_i \cdot \boldsymbol{S} = -\frac{\delta F}{\delta u_i}$ (mech. equilibrium equation)

$0 = \Delta\varphi = \frac{\delta F}{\delta \varphi}$ (electrostatics, charge free)

- Mechanical quantities:

u_i: mech. displ. in i direction

$\varepsilon_{ij} = \frac{1}{2}\left(\frac{\partial u_i}{\partial j} + \frac{\partial u_j}{\partial i}\right)$: mech. strain tensor

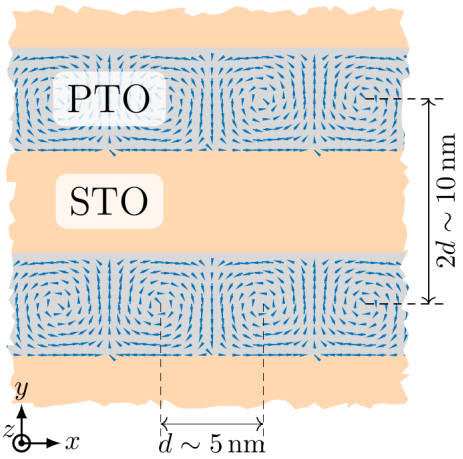

$$F = \iiint \Big(\overbrace{\alpha_{ij}P_iP_j + \alpha_{ijk\ell}P_iP_jP_kP_\ell + \alpha_{ijklmn}P_iP_jP_kP_\ell P_mP_n}^{f_{\mathrm{Landau}}} + \overbrace{\frac{1}{2}g_{ijkl}\frac{\partial P_i}{\partial x_j}\frac{\partial P_k}{\partial x_\ell}}^{f_{\mathrm{Grad}}} + \overbrace{\frac{1}{2}c_{ijkl}\varepsilon_{ij}\varepsilon_{kl} - q_{ijkl}\varepsilon_{ij}P_kP_\ell}^{f_{\mathrm{Elast}}} - \overbrace{\frac{1}{2}\kappa_b E_iE_i - E_iP_i}^{f_{\mathrm{E_{stat}}}} \Big)\,\mathrm{d}V$$

[2] T. Yang *et al.*, *Phys. Rev. Lett.*, vol. 124, no. 10, 2020.
[3] Q. Li *et al.*, *Nature*, vol. 592, no. 7854, 2021.

UNIVERSITÄT DUISBURG ESSEN

Offen im Denken

Phase Field Model

- Governing equations [1, 2]:

$\mu\ddot{P}_i + \gamma\dot{P}_i = -\frac{\delta F}{\delta P_i}$ (2nd-order TD-LGD equation)

$\rho\ddot{u}_i + \beta\rho\dot{u}_i = \nabla_i \cdot \boldsymbol{S} = -\frac{\delta F}{\delta u_i}$ (mech. equilibrium equation)

Coupled via electrostrictive effect

$0 = \Delta\varphi = \frac{\delta F}{\delta \varphi}$ (electrostatics, charge free)

- Mechanical quantities:

u_i: mech. displ. in i direction

$\varepsilon_{ij} = \frac{1}{2}\left(\frac{\partial u_i}{\partial j} + \frac{\partial u_j}{\partial i}\right)$: mech. strain tensor

$$F = \iiint \left(\overbrace{\alpha_{ij}P_iP_j + \alpha_{ijk\ell}P_iP_jP_kP_\ell + \alpha_{ijklmn}P_iP_jP_kP_\ell P_mP_n}^{f_{\mathrm{Landau}}} + \overbrace{\frac{1}{2}g_{ijkl}\frac{\partial P_i}{\partial x_j}\frac{\partial P_k}{\partial x_\ell}}^{f_{\mathrm{Grad}}} + \overbrace{\frac{1}{2}c_{ijkl}\varepsilon_{ij}\varepsilon_{kl} - q_{ijkl}\varepsilon_{ij}P_kP_\ell}^{f_{\mathrm{Elast}}} - \overbrace{\frac{1}{2}\kappa_b E_iE_i - E_iP_i}^{f_{\mathrm{E_{stat}}}} \right) \mathrm{d}V$$

[2] T. Yang *et al.*, *Phys. Rev. Lett.*, vol. 124, no. 10, 2020.
[3] Q. Li *et al.*, *Nature*, vol. 592, no. 7854, 2021.

UNIVERSITÄT DUISBURG ESSEN

Offen im Denken

Phase Field Model

- Governing equations [1, 2]:

$\mu\ddot{P}_i + \gamma\dot{P}_i = -\frac{\delta F}{\delta P_i}$ (2nd-order TD-LGD equation)

$\rho\ddot{u}_i + \beta\rho\dot{u}_i = \nabla_i \cdot \boldsymbol{S} = -\frac{\delta F}{\delta u_i}$ (mech. equilibrium equation)

$0 = \Delta\varphi = \frac{\delta F}{\delta \varphi}$ (electrostatics, charge free)

- Mechanical quantities:

u_i: mech. displ. in i direction

$\varepsilon_{ij} = \frac{1}{2}\left(\frac{\partial u_i}{\partial j} + \frac{\partial u_j}{\partial i}\right)$: mech. strain tensor

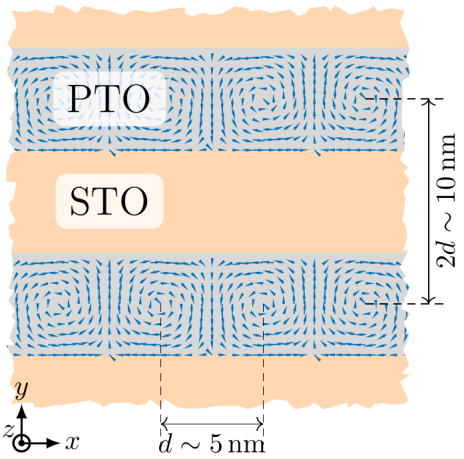

$$F = \iiint \left(\overbrace{\alpha_{ij}P_iP_j + \alpha_{ijk\ell}P_iP_jP_kP_\ell + \alpha_{ijklmn}P_iP_jP_kP_\ell P_mP_n}^{f_{\mathrm{Landau}}} + \overbrace{\frac{1}{2}g_{ijkl}\frac{\partial P_i}{\partial x_j}\frac{\partial P_k}{\partial x_\ell}}^{f_{\mathrm{Grad}}} + \overbrace{\frac{1}{2}c_{ijkl}\varepsilon_{ij}\varepsilon_{kl} - q_{ijkl}\varepsilon_{ij}P_kP_\ell}^{f_{\mathrm{Elast}}} - \overbrace{\frac{1}{2}\kappa_b E_iE_i - E_iP_i}^{f_{\mathrm{E_{stat}}}} \right) \mathrm{d}V$$

M. Degen | Bremen Workshop on Light Scattering 2026 | March, 17th 2026

[2] T. Yang *et al.*, *Phys. Rev. Lett.*, vol. 124, no. 10, 2020.
[3] Q. Li *et al.*, *Nature*, vol. 592, no. 7854, 2021.

UNIVERSITÄT DUISBURG ESSEN

Offen im Denken

Phase Field Model

- Governing equations [1, 2]:

$$\mu\ddot{P}_i + \gamma\dot{P}_i = -\frac{\delta F}{\delta P_i}$$

$$\rho\ddot{u}_i + \beta\rho\dot{u}_i = \nabla_i \cdot \boldsymbol{S} = -\frac{\delta F}{\delta u_i}$$

$$0 = \Delta\varphi = \frac{\delta F}{\delta \varphi}$$

- Small random initial polarization
  → Solving using TD-FEM

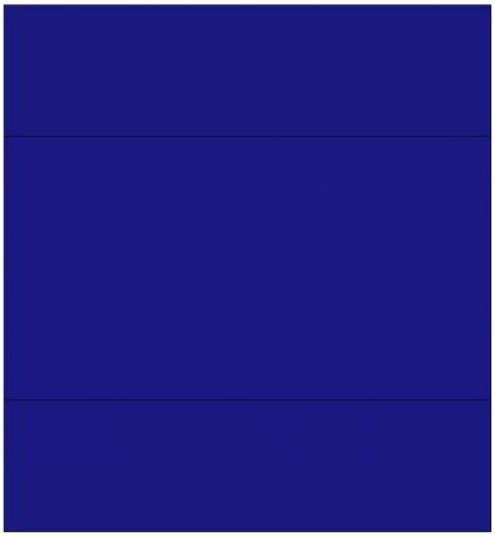

[2] T. Yang *et al.*, *Phys. Rev. Lett.*, vol. 124, no. 10, 2020.
[3] Q. Li *et al.*, *Nature*, vol. 592, no. 7854, 2021.

UNIVERSITÄT DUISBURG ESSEN

Offen im Denken

Phase Field Model

- Governing equations [1, 2]:

$$\mu\ddot{P}_i + \gamma\dot{P}_i = -\frac{\delta F}{\delta P_i}$$

$$\rho\ddot{u}_i + \beta\rho\dot{u}_i = \nabla_i \cdot \boldsymbol{S} = -\frac{\delta F}{\delta u_i}$$

$$0 = \Delta\varphi = \frac{\delta F}{\delta \varphi}$$

- Small random initial polarization
  → Solving using TD-FEM

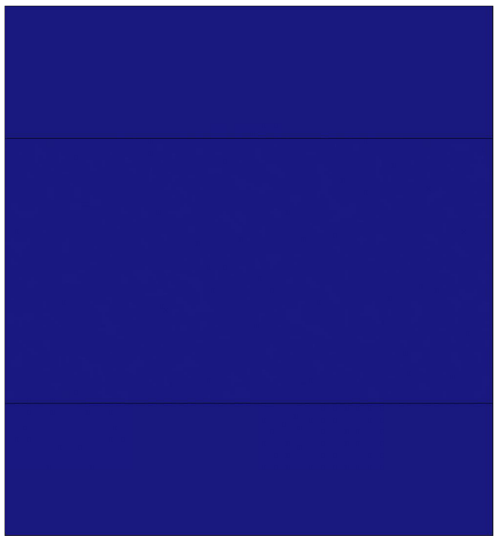

[2] T. Yang *et al.*, *Phys. Rev. Lett.*, vol. 124, no. 10, 2020.
[3] Q. Li *et al.*, *Nature*, vol. 592, no. 7854, 2021.

Torsional Rotator Model

- External electric field: excitation of collective modes in the sub-THz-regime

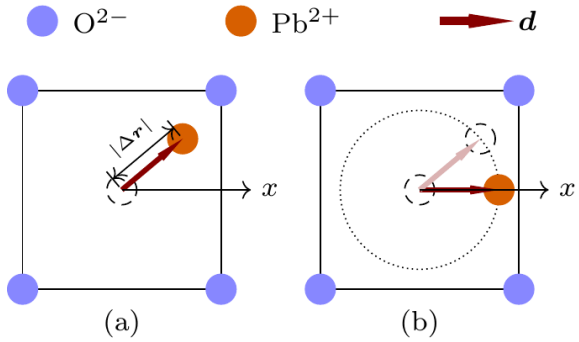

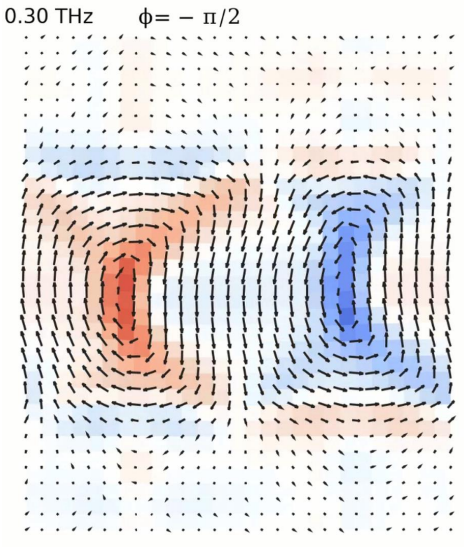

[3] Q. Li *et al.*, *Nature*, vol. 592, no. 7854, pp. 376–380, 2021.

Torsional Rotator Model

- Rotator model

$$\hat{\mathbf{I}}\ddot{\boldsymbol{\alpha}} = \mathbf{d}\times\mathbf{E} + \mu_0\boldsymbol{l}\times(\dot{\mathbf{d}}\times\mathbf{H})$$
$$\mathbf{d} = \mathbf{d}_0 + \delta\mathbf{d}(t); \quad \delta\mathbf{d} = \boldsymbol{\alpha}\times\mathbf{d}_0$$
$$\hat{\mathbf{I}}\delta\ddot{\mathbf{d}} = -\mathbf{d}_0\times(\mathbf{d}_0\times\mathbf{E})$$

$$\rightarrow \hat{\chi} = \begin{pmatrix} -\frac{d_{0y}^2}{\varepsilon_0\omega^2 I_z} & \cancel{\frac{d_{0y}d_{0x}}{\varepsilon_0\omega^2 I_z}} & 0 \\ \cancel{\frac{d_{0y}d_{0x}}{\varepsilon_0\omega^2 I_z}} & -\frac{d_{0x}^2}{\varepsilon_0\omega^2 I_z} & 0 \\ 0 & 0 & -\frac{d_{0x}^2+d_{0y}^2}{\varepsilon_0\omega^2 I_x} \end{pmatrix}$$

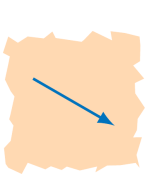

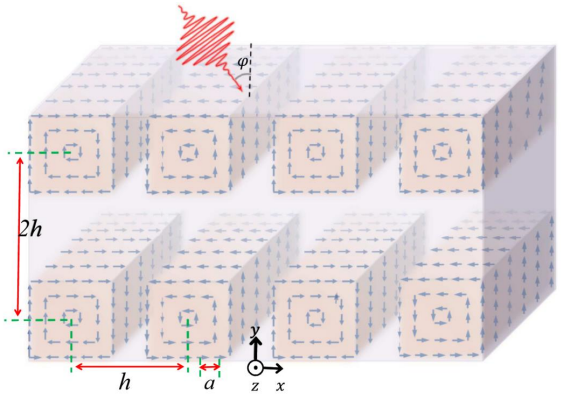

[4] R. Khomeriki *et al.*, *Phys. Rev. B*, vol. 109, no. 109, p. 045428, Jan. 2024.

$$\hat{\varepsilon} = \begin{pmatrix} \varepsilon_x & 0 & 0 \\ 0 & \varepsilon_y & 0 \\ 0 & 0 & \varepsilon_z \end{pmatrix}$$

Fourier series

$$\varepsilon_x = \varepsilon_y = \varepsilon_0 - \frac{\varepsilon_0\kappa^2}{4\,\omega^2}\left(1+\frac{4}{\pi}\cos\left(\frac{Q\,y}{2}\right)+\cdots\right)\left(1+\frac{4}{\pi}\cos(Q\,x)+\cdots\right)$$

Torsional Rotator Model

$$\hat{\boldsymbol{\varepsilon}} = \begin{pmatrix} \varepsilon_x & 0 & 0 \\ 0 & \varepsilon_y & 0 \\ 0 & 0 & \varepsilon_z \end{pmatrix}$$

- Wave equation:

$$\Delta\mathbf{E} - \nabla(\nabla \cdot \mathbf{E}) = -\frac{\omega^2 \hat{\boldsymbol{\varepsilon}} \cdot \mathbf{E}}{c^2 \varepsilon_0}$$

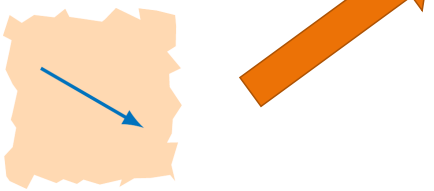

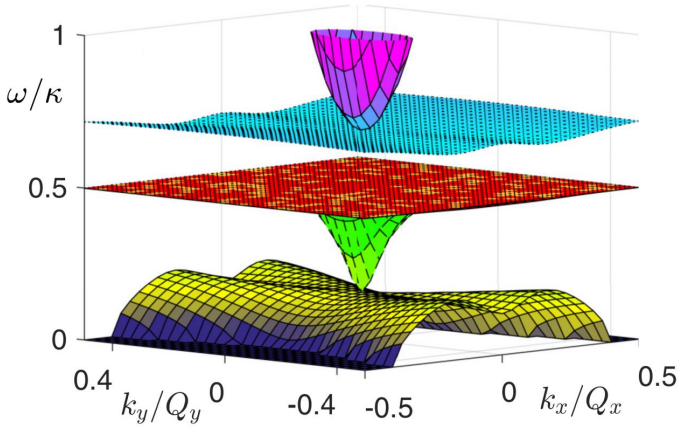

[4] R. Khomeriki *et al.*, *Phys. Rev. B*, vol. 109, no. 4, p. 045428, Jan. 2024.

Square and Circular Vortex Model

- **T**-matrix: relating expansion coefficients of incident and scattered field

$$T_n = -\frac{B_{1n} J_n'(k_0 r_2) - B_{2n} J_n(k_0 r_2)}{B_{3n} H_n^{(1)'}(k_0 r_2) - B_{4n} H_n^{(1)}(k_0 r_2)}$$

- Accounting for the vortex texture in $B_{i\,n}$
- Lattice sums: solving the scattering problem of a periodic structure

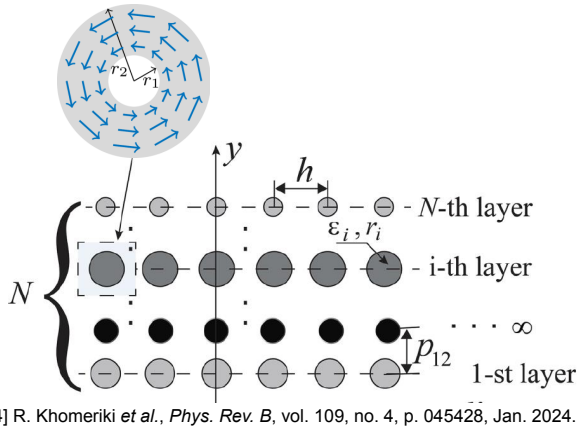

[4] R. Khomeriki *et al.*, *Phys. Rev. B*, vol. 109, no. 4, p. 045428, Jan. 2024.

[5] V. Jandieri *et al.*, *IEEE Trans. Antennas Propag.*, vol. 67, no. 4, pp. 2346-2378, Apr. 2019.

Square and Circular Vortex Model

- Comparison of the square and circular model

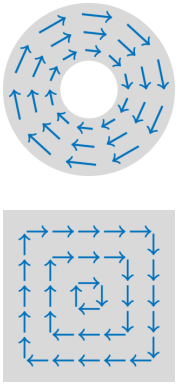

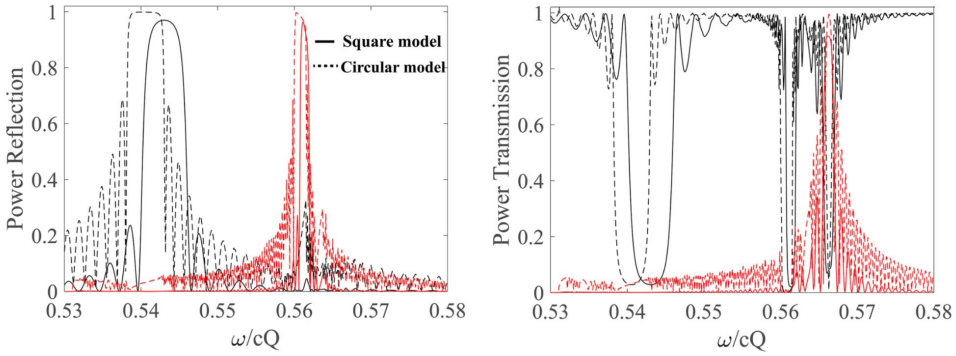

[4] R. Khomeriki *et al.*, *Phys. Rev. B*, vol. 109, no. 4, p. 045428, Jan. 2024.

UNIVERSITÄT DUISBURG ESSEN
Offen im Denken

Torsional Spring Model

Ground state: (local) energy minimum

External field: deflection

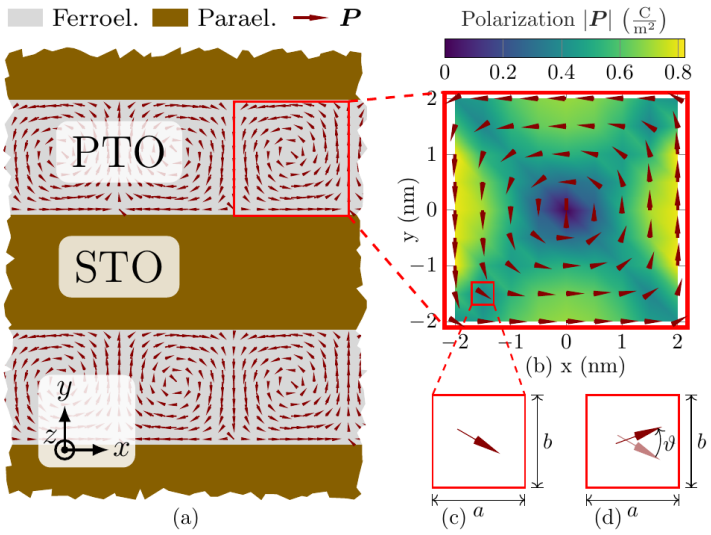

Torsional Spring Model

Ground state: (local) energy minimum

External field: deflection

Free energy: increases

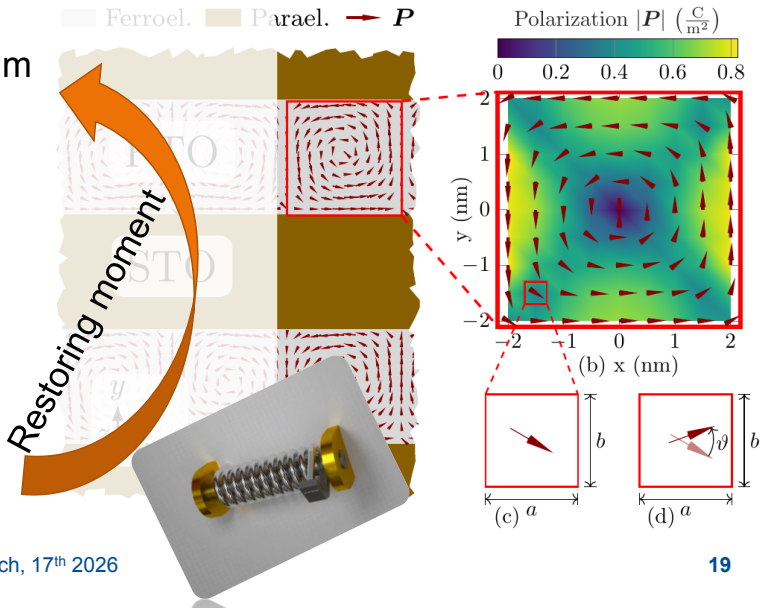

Torsional Spring Model

- Neglecting coupling (gradient energy terms)
- Crystal unit cell: $V = a\ b\ c$
- Moment of inertia as function of $\boldsymbol{P}$

$$\boldsymbol{P} = \frac{q_{\mathrm{eff}}\,\Delta\boldsymbol{r}}{V} \Rightarrow I_z = m_{\mathrm{Pb}}|\Delta\boldsymbol{r}|^2 = \frac{m_{\mathrm{Pb}}\,V^2}{q_{\mathrm{eff}}}|\boldsymbol{P}|^2$$

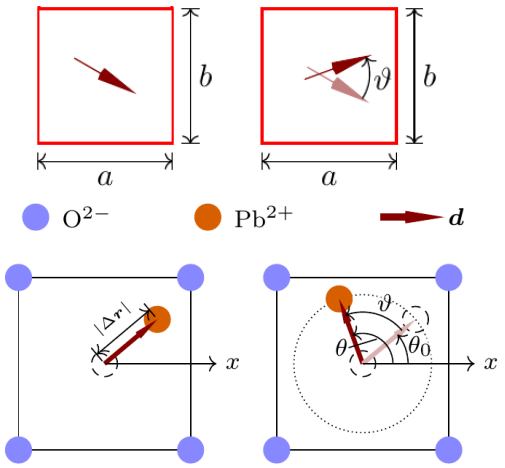

Torsional Spring Model

- Neglecting coupling (gradient energy terms)
- Crystal unit cell: $V = a\ b\ c$
- Moment of inertia as function of $\boldsymbol{P}$

$$\boldsymbol{P} = \frac{q_{\text{eff}}\,\Delta \boldsymbol{r}}{V} \Rightarrow I_z = m_{\text{Pb}}|\Delta \boldsymbol{r}|^2 = \frac{m_{\text{Pb}}\,V^2}{q_{\text{eff}}}|\boldsymbol{P}|^2$$

- Restoring torque: principle of virtual displacement

$$M_{\text{res}}(\vartheta_i) = \frac{F_{\vartheta_i} - F_{i-1}}{\vartheta_i - \vartheta_{i-1}}\frac{V}{V_c} \Rightarrow k = \frac{M_{res}(\vartheta_i) - M_{res}(\vartheta_{i-i})}{\vartheta_i - \vartheta_{i-1}}$$

$$I_z \frac{\partial^2 \vartheta}{\partial t^2} + C\frac{\partial \vartheta}{\partial t} + k\,\vartheta = M_{\text{d}}$$

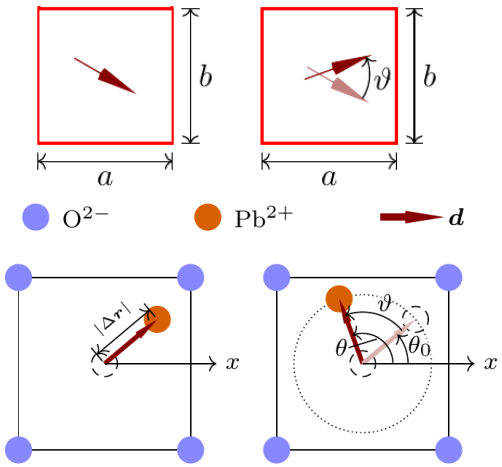

$$f_0 = 0.16\ \text{THz}\ \ldots 0.5\ \text{THz}$$

Perturbation Analysis

- Dependent variables: superposition of static and dynamic part

$$\mu\ddot{P}_i + \gamma\dot{P}_i = -\frac{\delta F}{\delta P_i} \qquad \rho\ddot{u}_i + \beta\rho\dot{u}_i = \nabla_i \cdot \boldsymbol{S} \qquad 0 = \Delta\varphi$$

$$\Rightarrow \quad P_i = \bar{P}_i + \tilde{P}_i \qquad u_i = \bar{u}_i + \tilde{u}_i \qquad \varphi = \bar{\varphi}_i + \tilde{\varphi}_i$$

$$\Rightarrow \quad \mu\ddot{\tilde{P}}_i + \gamma\dot{\tilde{P}}_i = -\frac{\delta\tilde{F}}{\delta\tilde{P}_i} \qquad \rho\ddot{\tilde{u}}_i + \beta\rho\dot{\tilde{u}}_i = \nabla_i \cdot \tilde{\boldsymbol{S}} \qquad 0 = \Delta\tilde{\varphi}$$

- $\tilde{F}$ is nonlinear

$\tilde{P}_i \ll \bar{P}_i$ → Floquet-BC → eigenmode analysis

$\tilde{P}_i \not\ll \bar{P}_i$ → Time-domain analysis → soliton excitation

UNIVERSITÄT DUISBURG ESSEN

Offen im Denken

Perturbation Analysis

- $\tilde{P}_i \ll \bar{P}_i$ → Floquet-BC → eigenmode analysis

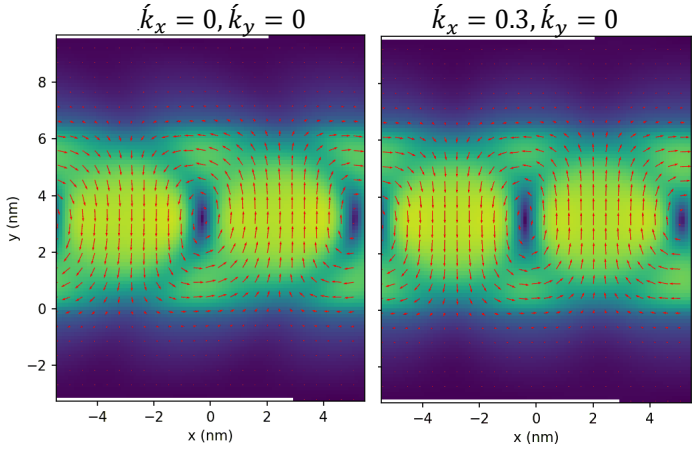

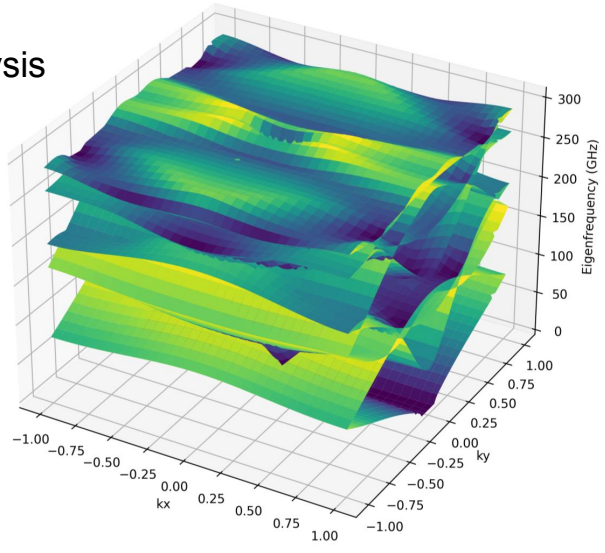

UNIVERSITÄT DUISBURG ESSEN

Offen im Denken

Conclusion and Outlook

- Emergence of topological vortex structures in PTO/STO layers
- Simplified models neglecting elastic effects and dipole coupling
- More sophisticated model including dipole coupling and elastic effects
  - Frequency domain: fast solution of dispersion relation for small perturbations
  - Time domain: including non linear effects
- Appear band-gaps in experimentally realizable structures?
- Analyzing non-linearity:
  - Modeling of solitons in ferroelectric vortex lattices
  - Quantifying Kerr-nonlinearities in sub-THz range
  - Experimental validation

Thank you for your attention!

Marvin Degen
University of Duisburg-Essen, Faculty of Engineering
General and Theoretical Electrical Engineering (ATE)
marvin.degen@uni-due.de

UNIVERSITÄT DUISBURG ESSEN

Offen im Denken